Optica Applicata, Vol. XII, No. 2, 1982

Evaluation of wave aberrations of objectives

Part III. Analysis of lateral shearing interferograms. Experimental results

BOGUSŁAWA DUBIK

Institute of Physics, Technical University of Wrocław, Wybrzeże Wyspiańskiego 27, 50-370 Wrocław, Poland.

In this paper a setup to test the objective is presented in which lateral shearing interferograms are produced. The method for analysis of the obtained interferograms as well as the block scheme of the programme calculating the objective wave aberrations are given. The experimental and numerical results are presented in Tables and graphs.

1. Introduction

In the previous papers [1, 2] of this cycle a generalized mathematical model of shearing interference was given. This model was used to determine the shape of the wavefront emerging from the objectives of small aberrations and to estimate these aberrations on the base of the respective shearing interferograms.

The distribution of interference fringes $\bar{N}(x, y)$ (distribution of the optical path difference between the interfering wavefronts) was determined analytically in the region of shearing interferogram by assuming that the analytical form of the wavefront $g(x, y)$ is known (the direct problem). By exploiting this result the inverse problem was solved, i.e., the wavefront shape was determined on the base of the information contained in the interferogram (the distribution of the interference fringes). The analysis of interferogram was performed along a chosen scanning lines $y = y_L$. The function $\bar{N}_L(x)$ describing the distribution of the interference fringes along this scanning line was determined and next the shape of the wavefront shape $g_L(x)$ for the given scanning $y = y_L$ was reconstructed. While solving the inverse problem is has been assumed that the wavefront is described by a power polynomial

$$g_L(x) = \sum_{j=0}^{M} a_{jL} x^j, \tag{1}$$

where L is the index of the scanning line and M is the polynomial degree not greater than 10. Thus, the function $\bar{N}_L(x)$ has the following form

$$\bar{N}_L(x) = \sum_{k=1}^{M+1} B_{kL} x^{(k-1)}, \tag{2}$$

where

$$\bar{N}_L(x) \equiv N_L(x)\lambda \tag{2a}$$

and $N_L(x)$ is a relative interference order of dark (or bright) interference fringe, λ is the light wavelength.

In the paper [2] the problems of the suitable choice of the reference sphere for the reconstructed wavefront and wave aberration calculation are discussed. In the first approximation the sphere passing through three given points of the wavefront was chosen as the reference sphere. Since such a sphere is highly sensitive to the incident local perturbations of the wavefront, an optimization of this sphere has been carried out with respect to the criterion of minimal rms of the wavefront deviation from the reference sphere. The results of the work [3] have been exploited, namely, that there exists a reference sphere for which the rms aberration reaches its minimum and simultaneously the Strehl definition takes its maximal value.

The paper [2] deals also with the problems connected with the wavefront reconstruction. In particular, it has been shown that the coefficients a_{jL} determining the wavefront $g_L(x)$ in (1) are calculated basing on the knowledge of the coefficients B_{kL} describing the distribution of the optical path difference $N_L(x)$ in (2) along the selected scanning line $y = y_L$. The coefficients are determined directly from the information contained in the shearing interferogram by using the method of approximation of the set of points $\{x_i, \bar{N}_L(x_i)\}$. The degree of the approximating polynomial is not known a priori and its choice affects significantly the approximation error. In particular, the approximating polynomial degree must be high enough to approximate correctly the real function – on one hand, but simultaneously not too high – on the other hand, since it is also expected to perform the smoothing of the empirical data. The criterion for the optimal degree of the approximating polynomial has been given in [2].

2. Experiment

The purpose of the experiment performed was to check the usefulness of the elaborated method of the shearing interferograms analysis. It has been applied to measure the wave aberration for the objectives corrected for infinity (for instance, the photographic or telescopic objectives). After having produced a series of lateral shearing interferograms for selected objectives the numerical analysis of the obtained interferogram were performed. For the objectives examined the wave aberrations were calculated and next the measured accuracies – estimated.

A single experiment results in a lateral shearing interferogram or a pair of such interferograms of mutually perpendicular lateral shifts of the respective wavefronts. Note that the analysis of a single interferogram requires the assump-

tion of symmetry of the wavefront [2]; no additional assumption about the wavefront being needed when two interferograms are analysed simultaneously. A pair of the lateral shearing interferograms is shown in Fig. 1, i.e., the so-called basic interferogram (Fig. 1a) and the additional one (Fig. 1b). These interferograms were performed in a setup, the scheme of which is shown in Fig. 2.

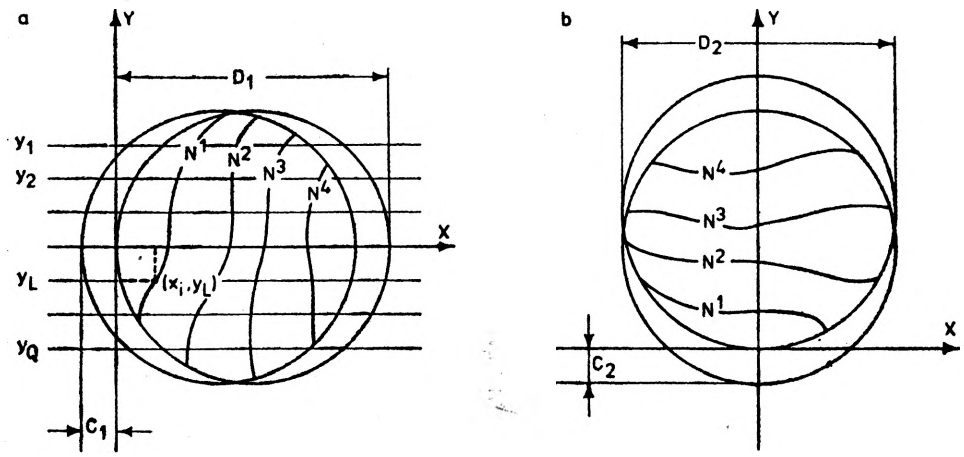

Fig. 1. Basic lateral shearing interferogram: C_1 — shift between the interfering wavefront in the x direction, D_1 — wavefront diameter, (x_i, y_i) — coordinates of the i-th fringe on the j-th scanning line, N^i — relative interference order of the i-th fringe (a). Additional lateral shearing interferogram: C_2 — shift between the interfering wavefronts in the y direction, D_2 — wavefront diameter (b)

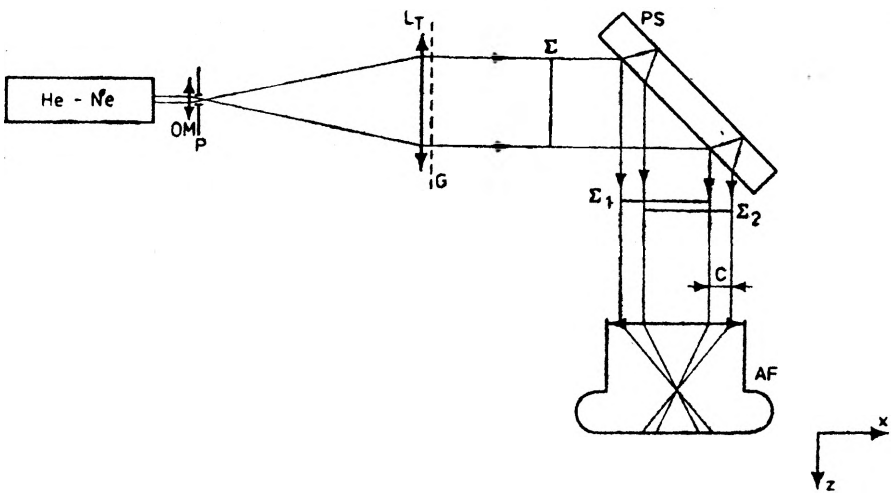

Fig. 2. Scheme of the measuring system to record the lateral shearing interferograms: Ne–He-Ne LG-600/PZO laser ($\lambda = 0.6328$ μm), OM — microscope objective, P — pinhole, L_T — lens tested, G — scanning grid, PS — shearing element, AF — photographic camera, Σ — wavefront examined, Σ_1, Σ_2 — interfering wavefronts, C — lateral shift between the wavefronts Σ_1 and Σ_2

The objective examined was positioned so that its focus be coincident with the pinhole P. A scanning grid G of elementary cell 2.5×2.5 mm produced of wires of 0.02 mm diameter was fastened on the objective. The grid G played an auxiliary role, i.e., being imaged sharp on the interferogram plane it gave the scanning lines and facilitated the accurate measurement of the lateral C between the interfering wavefronts Σ_1 and Σ_2. Independently, it proved to be helpful also in production of two interferograms of mutually perpendicular shifts. The examined wavefront Σ from the objective L_T was splitted by a plane-parallel plate PS into two wavefronts Σ_1 and Σ_2. The plate PS of the thickness $h = 20.2$ mm, and diameter $\Phi_p = 145$ mm, and with the refractive index $n = 1.5146$ is an element from the OCK-2 optical bench equipment. The interference effect of the separated wavefronts Σ_1 and Σ_2 was recorded in the image plane of the photographic camera AF.

For each of the examined objectives several measurements were made, while the shift C was changed (by changing the incidence angle of the wavefront Σ on the plate PS) or the objective defocussed by Δf (in order to obtain the suitable number of fringes in the interferogram region). When the additional interferogram was made the magnification was preserved exactly the same as that in the basic interferogram ($D_1 = D_2 \equiv D$). The same was true for the respective shifts ($C_1 = C_2 \equiv C$) of the interfering beams. Before recording both the interferograms the direction of the relative frequency density increase of the interference fringes has been determined. The coefficients $TK1$ and $TK2$ from [1] have been assumed to be equal to zero, since the shearing element was a plane-parallel plate. The remaining quantities, except for the light wavelength λ used in the measurements, were read out immediately from the interferograms. These were: the diameter of the wavefronts D, lateral shifts C between the interfering wavefronts, the position of the interference fringe midpoints x_i on particular scanning lines y_L, the coordinates of the scanning lines y_L, relative interference orders, N_L^i attributed to the particular interference fringes ($N_L^i \stackrel{\text{def}}{=} N_L(x_i)$). On the base of these data from the interferogram the magnification of the interferogram photo was estimated with respect to the real objective. The above data have been introduced to the programme ABCD elaborated in the Fortran language.

3. Software for numerical calculation

The programme ABCD consists of segments MASTER, APROX, FRONT, PION and OPTYM. The tasks (to be solved by the particular segments (blocks) of the programme) are listed below:

APROX: its task is to find the function $\bar{N}_L(x)$ describing the distribution of the optical path difference between the interfering wavefronts, i.e., to calculate the coefficients B_{kL} ($k = 1, \ldots, 11$, $L = 1, \ldots, Q$) in the expression (2). The basis for finding this function is the position of the midpoints of the interfer-

ence fringes $\{x_i\}$ on the shearing interferogram and the relative interference orders of those fringes $\{N_L^i\}$. Basing on the set of the points $\{(x_i, \bar{N}_L^i)\}$ this subroutine carries out the approximation of the function $\bar{N}_L(x)$ by using the least square method and exploiting the subroutine F4CFORPL from the ELWRO software library. The F4CFORPL subroutine enables the approximation of the given set of points by a power polynomial of the accepted degree. While choosing the optimal degree of the polynomial for the approximated set of points the method of optimization given in the previous article [2] of this cycle has been adopted. As a results of calculation by using the subroutine APROX the set of the desired coefficients $\{B_{kL}\}$ has been obtained.

FRONT: its task is to find the coefficients a_{jL} ($j = 1, \ldots, 10$, $L = 1, \ldots, Q$) describing the wavefront function $g_L(x)$ in (1). The solution of this task is based on the coefficients $\{B_{kL}\}$ calculated in subroutine APROX. The relations between the coefficients a_{jL} and B_{kL} are given in the first paper of this cycle [1].

PION: the task of this subroutine is to calculate the coefficients a_{0L} in the case when no symmetry of the wavefront is assumed, while the data from the scanning along the $x = 0$ line recorded on an additional shearing interferogram are exploited. In the case when for the calculation of the a_{0L} coefficients the assumption of wavefront symmetry is made, the coefficients a_{0L} are calculated by a subroutine in the MASTER programme.

MASTER: it plays the part of a controlling block performing the basic calculations. After obtaining the information from APROX and FRONT (or from PION) the programme MASTER calculates the wavefronts $g_L(x)$,

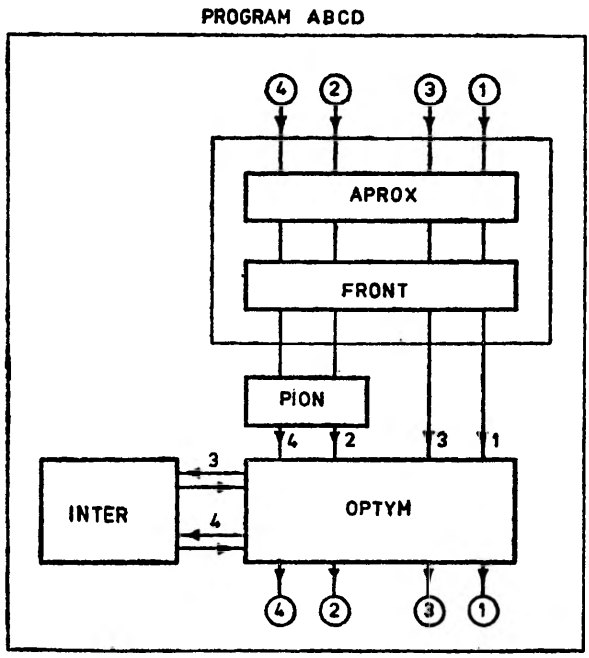

Fig. 3. Scheme of the ABCD programme operation in the versions 1, 2, 3 and 4

the reference spheres $S_L(x)$ and the wave aberrations $W_L(x)$ for particular lines of scanning $y = y_L$ $(L = 1, \ldots, Q)$.

OPTYM: its plays the part of a block performing the optimization of the aberrations $W_L(x)$ obtained from MASTER. As a result of its calculation optimized wave aberration function $W'_L(x)$ is obtained [2].

INTER: its function consists in finding a two-dimensional wavefront function $g(x, y)$ on the base of the coefficients $a_{jL}(j = 0, \ldots, 10, L = 1, \ldots, Q)$ describing the one-dimensional wavefront functions (a_{jL} have been calculated previously in the FRONT block) and in calculating the reference sphere and wavefront aberrations. The two-dimensional model of the wavefront has been discussed more accurately in [4]. For the analysis of lateral shearing interferogram the ABCD programme may function in four versions. The block scheme of the ABCD programme is shown in Fig. 3.

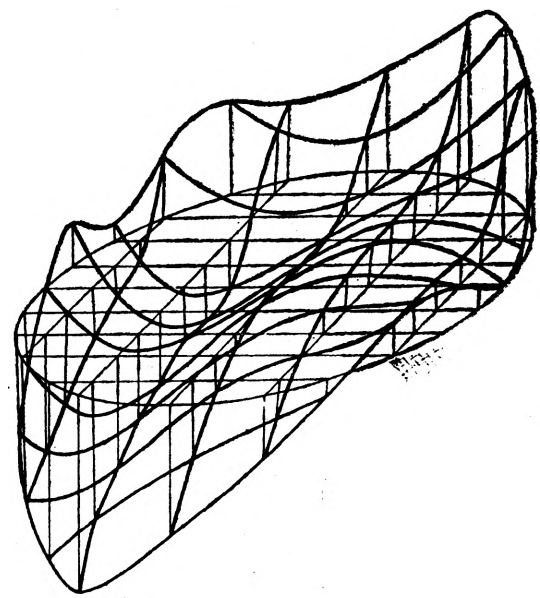

Fig. 4a. Wave aberrations of the L_{II} objective calculated with respect to the reference sphere passing through the three given wavefront points (non-optimal aberrations)

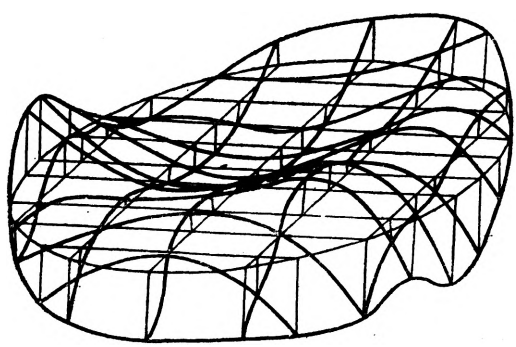

Fig. 4b. Wave aberrations of the L_{II} objective calculated with respect to the optimal reference sphere (optimal aberrations)

4. Results of calculations

The results of the calculation have been presented in the form of graphs, contour lines (for constant values of wave aberrations) and tables with numerical data. The results have been compiled to illustrate the performance of the suggested measurement method at its particular stages.

In Fig. 4 a, b the effect of functioning of the optimal reference sphere is shown by presenting the wave aberrations of the objective calculated with respect to the reference sphere passing through the three given points of the wavefront (we will call them non optimal aberrations) and the aberrations calculated with respect to the optimal reference sphere (optimal aberrations). The effect of compensation of the aberration slope with respect to the coordinate system may be seen distinctly.

Taking the objective L_{II} as an example, the wave aberrations obtained under assumption of the wavefront symmetry for the examined objective (the result of basic interferogram analysis) are shown in Fig. 5a, while those without this assumption (resulting from simultaneous analysis of basic and additional interferograms) are given in Fig. 5b. In all the figures the values of the aber-

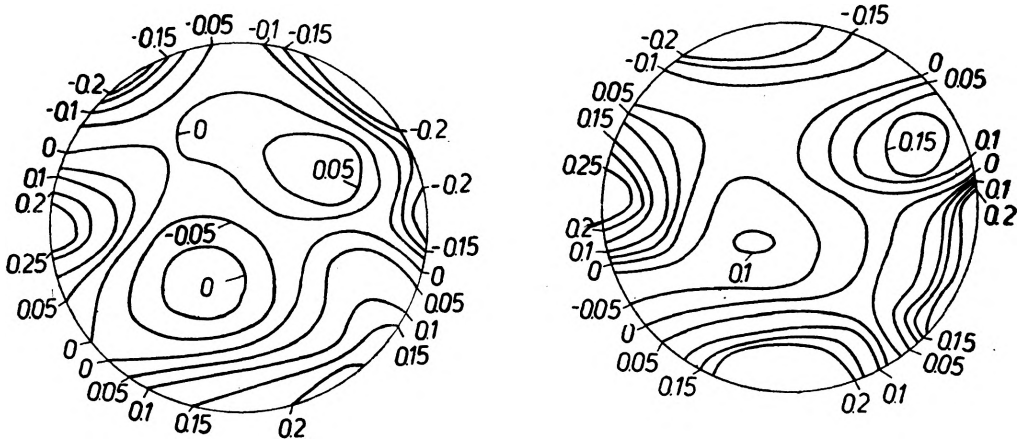

Fig. 5. Optimal wave aberrations for the L_{II} objective obtained under assumption of the symmetry of the wavefront coming from the objective (a). Optimal wave aberrations of the objective lens L_{II} obtained without assumption of the wavefront symmetry (b)

rations are given in the λ-units. In Fig. 6 the optimal wave aberrations are shown for the objective L_I obtained by using a one-dimensional model of the wavefront (Fig. 6a) and the optimal aberrations of this objective obtained by employing a two-dimensional model of the wavefront (Fig. 6b) [4].

Tables 1–3 contain the parameters characterizing the examined objective (Φ — diameter of the objective, f — focal length of the objective) and the parameters determining the measuremental conditions (C — the shift of the

interfering wavefronts, Δf — defocussing objective, PR_{max} — maximal number of fringes on the interferogram, Q — considered number of scanning lines). In each of the tables the parameters mentioned above are listed together with the quantities characterizing the reconstructed wavefront and the wave aberrations calculated as the respective rms. For the whole exit pupil of the examined objective the respective rms are denoted as follows:

$$
\begin{aligned}
S_{g_L} &= \sqrt{\frac{1}{Li}\sum_{j,L} g_L^2(x_j)}, \\
S_{W_L} &= \sqrt{\frac{1}{Li}\sum_{j,L} W_L^2(x_j)}, \\
S_{W'_L} &= \sqrt{\frac{1}{Li}\sum_{j,L} W'^2_L(x_j)}, \\
S_g &= \sqrt{\frac{1}{Li}\sum_{j,k} g^2(x_j, y_k)}, \\
S_{W'} &= \sqrt{\frac{1}{Li}\sum_{j,k} W'^2(x_j, y_k)},
\end{aligned}
\tag{3}
$$

where Li is the considered number of the points in the whole pupil.

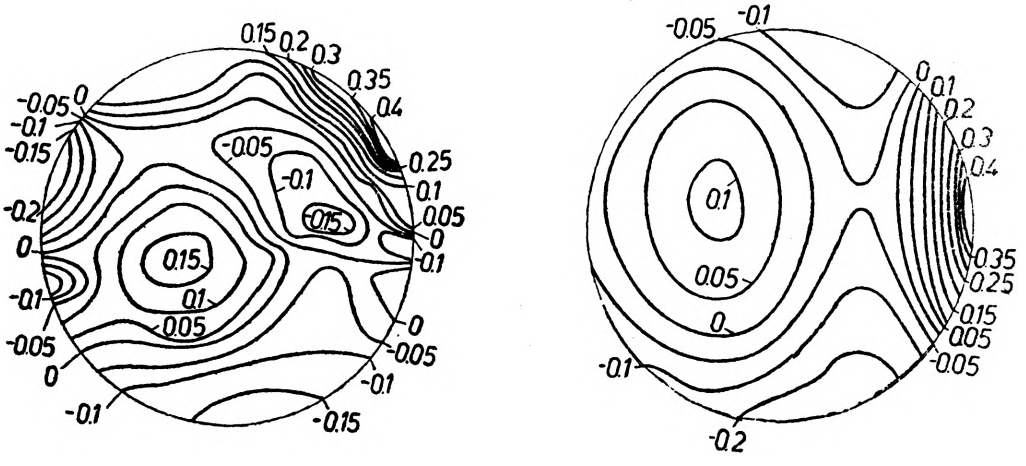

Fig. 6. Optimal wave aberrations of the L_I objective obtained on the base of one-dimensional wavefront model (a). Optimal wave aberrations of the L_I objective obtained on the base of two-dimensional wavefront model (b)

Table 1. L_I objective parameters ($f = 400$ mm, $\Phi = 65$ mm) and the obtained measurement results

		$L_I(a)$	L_I(b)	$L_I(c)$	$L_I(d)$	$L_I(e)$	av	$\Delta(\text{av})_{\max}$	σ
C	[mm]	9.52	9.90	14.38	15.36	15.48			
Δf	[mm]	3.00	1.00	2.00	3.00	1.00			
Q		11	11	13	13	11			
$PR_{\max}$		19	8	16	26	10			
S_{g_L}	[λ]	10.507	4.014	6.950	10.320	3.830			
S_{W_L}	[λ]	0.252	0.165	0.227	0.219	0.193	0.211	0.047	0.033
δS_{W_L}	[%]	19.360	22.040	7.470	3.690	8.510	12.220		
$S_{W'_L}$	[λ]	0.130	0.100	0.104	0.106	0.101	0.108	0.021	0.012
$\delta S_{W'_L}$	[%]	19.630	7.560	3.600	2.210	6.450	7.890		
S_g	[λ]	10.498	4.005	6.905	10.313	3.811			
$S_{W'}$	[λ]	0.098	0.089	0.068	0.097	0.090	0.089	0.021	0.012
$\delta S_{W'}$	[%]	10.940	1.010	23.670	9.580	2.140	9.470		
ΔS_g	[%]	0.080	0.220	0.650	0.060	0.520	0.310		
$\Delta S_{W'}$	[%]	27.520	11.270	42.830	8.760	11.350	20.350		

Table 2. L_{II} objective parameters ($f = 500$ mm, $\Phi = 50$ mm) and the obtained measurement results

		$L_{II}(a)$	$L_{II}(b)$	$L_{II}(c)$	$L_{II}(d)$	$L_{II}(e)$	av	$\Delta(\text{av})_{\max}$	σ
C	[mm]	5.83	6.08	7.38	15.70	15.77			
Δf	[mm]	6.00	10.00	3.75	3.75	5.25			
Q		17	17	9	9	9			
$PR_{\max}$		10	16	8	12	16			
S_{g_L}	[λ]	6.633	10.343	4.134	3.441	5.052			
S_{W_L}	[λ]	0.233	0.195	0.142	0.122	0.062	0.151	0.088	0.066
δS_{W_L}	[%]	54.400	29.080	5.660	19.050	58.760	33.390		
$S_{W'_L}$	[λ]	0.086	0.081	0.061	0.060	0.053	0.068	0.017	0.014
$\delta S_{W'_L}$	[%]	25.440	19.000	10.230	11.400	22.800	17.770		
S_g	[λ]	6.645	10.354	4.137	3.454	5.063			
$S_{W'}$	[λ]	0.057	0.051	0.045	0.045	0.026	0.044	0.019	0.011
$\delta S_{W'}$	[%]	27.420	13.930	0.440	0.900	42.250	16.990		
ΔS_g	[%]	0.180	0.110	0.060	0.390	0.220	0.190		
$\Delta S_{W'}$	[%]	40.900	46.240	31.450	29.760	69.040	43.510		

The quantities S_{g_L}, S_{W_L}, $S_{W'_L}$ concern the one-dimensional model, while the quantities S_g, S_W, $S_{W'_L}$ concern the two-dimensional model, ($g(x, y)$ is the two-dimensional wavefront function and $W'(x, y)$ is the two-dimensional function of optimal wave aberrations.

Table 3. Comparison of results obtained for L_{II} objective with (**) and without (*) the assumption of the wavefront symmetry

	$L_{II}(a)$		$L_{II}(b)$	
	*	**	*	**
C	5.83		6.08	
Δf	6.00		10.00	
Q	17		17	
$PR_{\max}$	10		16	
S_{g_L} [λ]	6.420	6.633	10.351	10.343
Δ_{g_L} [%]	—	3.330	—	0.070
S_{W_L} [λ]	0.227	0.233	0.163	0.195
ΔW_L [%]	—	2.460	—	19.300
$S_{W'_L}$ [λ]	0.092	0.086	0.086	0.081
$\Delta W'_L$ [%]	—	7.140	—	6.000

ΔS_g and $\Delta S_{W'}$ denote the following expressions:

$$\Delta S_g = \frac{|S_{g_L} - S_g|}{\frac{1}{2}(S_{g_L} + S_g)} \, 100\ \%, \qquad \Delta S_{W'} = \frac{|S_{W'_L} - S_{W'}|}{\frac{1}{2}(S_{W'_L} - S_{W'})} \, 100\ \%. \tag{4}$$

The quantities Δ_{g_L}, Δ_{W_L}, $\Delta_{W'_L}$ represent the ratio of the differences of the corresponding rms of S_{g_L}, S_{W_L}, $S_{W'_L}$ for the case with the rotational symmetry of the wavefront and without the wavefront symmetry, to the respective rms for the case without wavefront symmetry. The above quantities are expressed in percent. Also the quantities δS_{W_L}, $\delta S_{W'_L}$, $\delta S_{W'}$ which denote the deviation of the rms of S_{W_L}, $S_{W'_L}$, $S_{W'}$ from the average value are given in percent; the average values are denoted by av, the maximal deviation from the average value by $\Delta(\mathrm{av})_{max}$ and the variance by σ.

5. The measurement accuracy

For several reasons the determination of the measurement accuracy for wave aberrations from an interferogram is by no means a simple task. The wave aberrations are measured indirectly by measuring the position of the fringes on the interferogram, the dependence between the aberration and the quantities measured directly being very complex. Moreover, the shape and the position of the fringes are affected by some incidental deformations of the interfering wavefronts occurring during their free propagation in the interferometer. These deformations may be due to gradients of refractive index in the air

within the interferometer (caused, in turn, by the temperature gradients) air motions and the like. The shearing element is another source of errors (systematic errors). The estimation of the influence of these errors on the accuracy of the aberration measurement is difficult, as (the optimal reference sphere in each measurement being fitted to the reconstructed wavefront) some components of the deformation (namely, both the shift and the wavefront slope with respect to the chosen coordinate system as well as the wavefront curvature) are compensated and have no influence on the result of the aberration measurement. Thus, only the deformation terms higher than second one introduce the errors to the measured wave aberrations.

The total measurement error of the wave aberration estimation consists of the random, systematic and approximation errors.

Random errors: The errors of this type occur both at the recording stage and at the stage of interferogram analysis. The wavefront in the ineterferometer is subject to the undesired deformations in the free propagation space. Hence, the influence of the sources of these deformations (temperature gradients, air fluctuations in the interferometer) should be restricted to minimum.

The random errors occurring during the analysis of interferogram depend on the accuracy of interference fringe midpoint localization.

In this work a method of interference fringe midpoint determination (directly from the photos) was applied. The position of the fringe midpoints may be measured with the help of an accurate millimeter scale. The accuracy of the midpoint coordinate determination depends upon the accuracy of visual localization of the fringe midpoint, while the uncertainty of this localization depends upon the spacing between the fringes (i.e., upon the interference fringe width). For the small interfringe spacings the localization accuracy is restricted by the accuracy of the coordinate measurement with the help of the millimeter scale. Thus, some care should be taken that the number of fringes in the interferogram be optimal, i.e., not too high, thus that the fringes be not too dense, and too low in order the fidelity of the optical path difference reconstruction in the interferometer be not restricted [5]. In the case of the interferograms analysed in this work the fringe localization accuracy obtained from a single measurement was 5–6%. For such a fringe accuracy and external measuring conditions (interferometer without housing protecting against the temperature gradient and the air fluctuations) a satisfying repeatability of the measurement results is obtained. When comparing the results obtained from different interferograms (but for the same objective) the maximal deviations of the wave aberrations obtained at the same points in the exit pupil of the examined objective did not exceed $\pm 0.03\ \lambda$. The rms deviation did not exceed the value of 0.015λ for all the points considered in the exit pupil. The values of the wave aberration averaged over the whole exit pupil and obtained from different interferometers for each of the examined objectives are given in Tables 1 and 2.

Systematic errors: In the measurement method used in this work a systematic error is introduced by the shearing element, i.e., by the plane-parallel plate.

Since this error cannot be eliminated, it should be minimized by using the shearing element of the highest quality, so that the systematic errors be much less than the aberrations measured. In the case of the measurements performed in this work the error due to the plane-parallel plate is estimated not to exceed $0.01\,\lambda$.

Approximation error: In the presented measurement method two kinds of approximations were introduced. One of them concerned the wavefront symmetry, i.e., it was assumed that the wavefront along the $x = 0$ was the same as that along the $y = 0$ line. This assumption gave a possibility of measuring the wave aberrations from only one (basic) interferogram. The results given in Tables 1 and 2 were obtained under the above assumption. In the case when this assumption was not used two (basic and additional) interferograms had to be analysed. The results of analysis of two interferograms are listed in Table 3 together with the results of the respective results of a single-interferogram analysis. As may be seen the error due to the assumed wavefront symmetry is of order of 8 % for the aberration averaged over the whole exit pupil of the examined objective (for different objectives this error may be different). Another approximation introduced to the measurement method concerned the two-dimensional description of wavefront on the base of one-dimensional descriptions obtained previously. The two-dimensional description of the wavefront necessitates the introduction of an additional approximation which results in an excessive smoothing at the wavefront and in the errors of aberration estimation. The result obtained is due to the approximating programme used. The errors of this approximation are of order of 50% (Tables 1 and 2). These errors may be considerably reduced by applying a suitable criterion for the choice of the optimal degree of the wavefront approximating polynomial. The applied criteria, well functioning in the case of optical path difference approximation from the lateral shearing interferogram, do not work good enough in the case of the approximation discussed. This is due to the fact that the approximated quantities are small and differ from one another by several orders of magnitude. It may be expected that the finding of the suitable criterion for approximating polynomial degree will allow to reconstruct the wavefront more faithfully than it was achieved so far.

The total error of the method is a sum of the incidental and systematic errors combined with those coming from the used approximations. Thus, the error of the method with the additional interferogram does not exceed $0.04\,\lambda$ at an arbitrary point of the exit pupil of the objective examined. The average error in the measured aberration across the whole pupil is usually less than 0.025λ. When using the method without additional interferogram the average error is greater due to the error of approximating procedure used. The latter is different for different objectives being greater for objectives of greater aberrations. The computer errors, being of order of $10^{-4}\lambda$, are negligible.

From the examinations carried out it follows that under the present measurement conditions and using the elaborated computer programme the aberra-

tion distribution in the objective exit pupil may be measured with an absolute accuracy of 0.04 λ (for hand scanning, visual method of interference fringe localization and an uncased measuring system). It is expected that, by employing a cased-type interferometer and an accurate (automatic) scanning device (enabling more accurate localization of the interference fringe midpoints) as well as by introducing into the numerical calculation programme the corrections taking account of the systematic errors of the shearing element, the wave aberrations may be estimated with the accuracy better than 0.01 λ.

References

[1] DUBIK B., Optica Applicata **10** (1980), 227–236.
[2] DUBIK B., Optica Applicata **9** (1981),
[3] PIETRASZKIEWICZ K., J. Opt. Soc. Am. **69** (1979), 1045–1046.
[4] DUBIK B., Optica Applicata **9** (1979), 285–289.
[5] KOWALIK W., Doctor's Thesis, Technical University of Wrocław, Institute of Physics, Wrocław 1974.

Received June 15, 1981

Определение волновых аберраций объективов.
Часть III. Анализ интерферограммы поперечный ширинг.
Результаты эксперимента

Представлена система для тестирования объективов, в которой выполнены интерферограммы поперечный ширинг. Представлен способ анализа полученных интерферограмм, а также дана блок-схема вычислительной программы, рассчитывающей волновые аберрации объективов. Полученные экспериментально-вычислительные результаты приведены в таблицах, а также на графиках. Обсуждены точности измерений.